Sympathetic Nerve Sprouting, Electrical Remodeling, and Increased Vulnerability to Ventricular Fibrillation in Hypercholesterolemic Rabbits

Yen-Bin Liu, Chau-Chung Wu, Long-Sheng Lu, Ming-Jai Su, Chii-Wann Lin, Shien-Fong Lin, Lan S. Chen, Michael C. Fishbein, Peng-Sheng Chen and Yuan-Teh Lee

Circ. Res. 2003;92;1145-1152; originally published online Apr 24, 2003;
DOI: 10.1161/01.RES.0000072999.51484.92
Circulation Research is published by the American Heart Association. 7272 Greenville Avenue, Dallas, TX 72514
 Print ISSN: 0009-7330. Online ISSN: 1524-4571

Sympathetic Nerve Sprouting, Electrical Remodeling, and Increased Vulnerability to Ventricular Fibrillation in Hypercholesterolemic Rabbits

Yen-Bin Liu, Chau-Chung Wu, Long-Sheng Lu, Ming-Jai Su, Chii-Wann Lin, Shien-Fong Lin, Lan S. Chen, Michael C. Fishbein, Peng-Sheng Chen, Yuan-Teh Lee

Abstract—Whether hypercholesterolemia (HC) can induce proarrhythmic neural and electrophysiological remodeling is unclear. We fed rabbits with either high cholesterol (HC, n=10) or standard (S, n=10) chows for 12 weeks (protocol 1), and with HC (n=12) or S (n=10) chows for 8 weeks (protocol 2). In protocol 3, 10 rabbits were fed with various protocols to observe the effects of different serum cholesterol levels. Results showed that the serum cholesterol levels were 2097±288 mg/dL in HC group and 59±9 mg/dL in S group for protocol 1 and were 1889±577 mg/dL in HC group and 50±21 mg/dL in S group for protocol 2. Density of growth-associated protein 43– (GAP43) and tyrosine hydroxylase– (TH) positive nerves in the heart was significantly higher in HC than S in protocol 1. Compared with S, HC rabbits had longer QTc intervals, more QTc dispersion, longer action potential duration, increased heterogeneity of repolarization and higher peak calcium current (I_{Ca}) density (14.0±3.1 versus 9.1±3.4 pA/pF; $P<0.01$) in protocol 1 and 2. Ventricular fibrillation was either induced or occurred spontaneously in 9/12 of hearts of HC group and 2/10 of hearts in S group in protocol 2. Protocol 3 showed a strong correlation between serum cholesterol level and nerve density for GAP43 ($R^2=0.94$; $P<0.001$) and TH ($R^2=0.91$; $P<0.001$). We conclude that HC resulted in nerve sprouting, sympathetic hyperinnervation, and increased I_{Ca}. The neural and electrophysiological remodeling was associated with prolonged action potential duration, longer QTc intervals, increased repolarization dispersion, and increased ventricular vulnerability to fibrillation. **(*Circ Res*. 2003;92:1145-1152.)**

Key Words: arrhythmia ■ lipids ■ ion channels ■ nervous system ■ pathology

Lipid-lowering interventions have been shown to reduce coronary events and all causes of mortality.[1–3] It is possible that some of the beneficial effects of lipid-lowering therapy can be attributed to the reduction of ventricular arrhythmias and sudden death.[1,3] De Sutter et al[4] performed an observational study in patients with coronary artery diseases and implantable cardioverter-defibrillators (ICD). Using the ICD records, the authors documented that the use of lipid-lowering drugs is associated with a reduction of recurrences of ventricular arrhythmias. The Kaplan-Meier curve of arrhythmia-free survival for patients with and without lipid-lowering drug therapy started to diverge within 1 to 2 months of follow-up. The magnitude and the speed of antiarrhythmic action cannot be explained by the reversal of atherosclerosis.[5] Previous studies have demonstrated that electrical remodeling occurs in diseased ventricles, and that these remodeling processes may contribute to the occurrence of ventricular arrhythmia.[6] In addition to electrical remodeling, neural remodeling in the form of sympathetic nerve sprouting may also result in ventricular arrhythmias in diseased human hearts and in animal models of sudden death.[7,8] Because cholesterol is important in synaptogenesis in the central nervous system,[9] it is possible that elevated serum cholesterol may promote neural remodeling in the peripheral nervous system. Therefore, we hypothesize that hypercholesterolemia (HC) can induce proarrhythmic neural and electrophysiological remodeling in the heart. The purpose of the present study was to use a rabbit model of HC to test this hypothesis.

Materials and Methods

Three-month-old New Zealand White rabbits were used for the study. The rabbits in protocol 1 were supplied by a vendor in Taipei, Taiwan, Republic of China. Rabbits in protocols 2 and 3 were obtained from a USDA-licensed commercial rabbit vendor in Southern California.

Original received October 24, 2002; resubmission received March 12, 2003; revised resubmission received April 9, 2003; accepted April 10, 2003.

From the Division of Cardiology, Department of Internal Medicine (Y.-B.L., C.-C.W., Y.-T.L.), National Taiwan University Hospital and National Taiwan University School of Medicine; Departments of Pharmacology (L.-S.L., M.J.S.) and Biomedical Engineering (C.-W.L.), National Taiwan University School of Medicine, Taipei, Taiwan; Division of Cardiology, Department of Medicine (Y.-B.L., S.-F.L., P.-S.C.), Cedars-Sinai Medical Center; Department of Neurology (L.S.C.), Children's Hospital and USC Keck School of Medicine; and Department of Pathology and Laboratory Medicine (M.C.F.), David Geffen School of Medicine, UCLA, Los Angeles, Calif.

Correspondence to Yuan-Teh Lee, MD, PhD, Division of Cardiology, Department of Internal Medicine, National Taiwan University Hospital, 7, Chung-Shan South Road, Taipei, 10016, Taiwan, Republic of China. E-mail ytlee@ha.mc.ntu.edu.tw; and Peng-Sheng Chen, MD, Division of Cardiology, Department of Medicine, Cedars-Sinai Medical Center, Room 5342, 8700 Beverly Blvd, Los Angeles, CA 90048. E-mail chenp@cshs.org

Circulation Research **is available at http://www.circresaha.org** **DOI: 10.1161/01.RES.0000072999.51484.92**

Protocol 1

This protocol was conducted in the vivarium of National Taiwan University School of Medicine, Taipei, Taiwan. Rabbits were fed with high fat and cholesterol chow (HC group, n=10) or standard chow (S group, n=10) for 12 weeks. Purina 5321 was used as standard rabbit chow. In HC chow, 40% of the total energy source was derived from 0.5% cholesterol (Wako Co) and 10% coconut oil (Yeali Co). In each group, 3 rabbits were male and 7 rabbits were female with bilateral oophorectomy.

Twelve-Lead Electrocardiographic Study

Twelve-lead surface electrocardiograms (ECGs) were performed in 6 rabbits of each group at 2-week intervals for 12 weeks. QT interval was measured manually. QT dispersion was defined as the difference between the longest and the shortest QT interval in the 12-lead ECG. The QTc was the QT divided by the square root of the RR interval in seconds.

Isolated Rabbit Heart Preparation and Electrophysiological Study

Rabbits were anesthetized. The hearts were quickly removed and Langendorff perfused with Tyrode's solution at room temperature (25° to 28°C). The Tyrode's solution had the following composition (in mmol/L): 125 NaCl, 4.5 KCl, 0.25 $MgCl_2$, 24 $NaHCO_3$, 1.8 NaH_2PO_4, 1.8 $CaCl_2$, and 5.5 glucose. The pH was maintained at 7.4, and the solution was continuously oxygenated with 95% O_2 and 5% CO_2. Electrical stimuli were delivered through the bipolar catheter with a rectangular pulse of 2-ms duration and 2 mA current for both S_1 and S_2. The vulnerability to ventricular tachyarrhythmias was tested with a single S_2 given after 8 S_1 at a cycle length of 600 ms on both left and right ventricles. The initial S_1-S_2 interval was 480 ms, which was decreased in 20 ms steps for coupling interval >300 ms and in 10-ms steps for coupling interval <300 ms until S_2 failed to capture or induce ventricular fibrillation.

Whole-Cell Clamping Study for Calcium Current Measurement

Whole-cell clamping study of cardiomyocytes was performed as previously described.[10] Briefly, 3 hearts of each group were retrogradely perfused with Ca^{2+}-free Tyrode's solution at 37°C for 5 minutes, followed by enzymatic digestion. Afterward the hearts were perfused with Kraftbruhe (KB) solution. Tissues from the left ventricle were dispersed in KB solution at room temperature (≈25°C). Cardiomyocytes were then transferred to a chamber mounted on an inverted microscope. Under whole-cell configuration, glass microelectrodes with an input resistance between 2 to 5 MΩ were used to record currents at room temperature with a Dagon 8900 amplifier. We added Cs^+ in both pipette and bath solution to eliminate the potassium current. A two-step depolarization protocol was used to study I_{Ca}. After depolarization to −40 mV for 100 ms, I_{Ca} was evoked by a second 300-ms depolarization to a test potential between −30 to 60 mV. The amplitude of I_{Ca} was measured as the peak amplitude of inward current. Data were then converted to current densities (pA/pF) according to cell capacitance.

Immunocytochemical Study

Ventricular tissues of rabbit hearts were fixed by 4% formalin for 1 hour followed by 70% alcohol for more than 48 hours after electrophysiological studies. Ventricles were cross-sectioned from apex to base. Three sections of each heart were used for immunocytochemical studies. Details of the staining techniques have been published elsewhere.[8,11] Briefly, we used anti–growth associated protein 43 (GAP43) and anti–tyrosine hydroxylase (TH) antibodies (monoclonal mouse anti-GAP43 and anti-TH, respectively, 1:50 dilution; Chemicon International, Inc) for immunocytochemical staining. GAP43, a protein expressed in the growth cones of sprouting axons,[12] is a marker for nerve sprouting. TH is a marker of sympathetic nerves.[13] We determined nerve density by a computer-assisted image analysis system (Image-Pro Plus 4.0). The computer automatically detected the stained nerves in these fields by their brown color (Figure 1A-a) and then labeled these nerves with a red color on the computer screen (Figure 1A-b). The computer then calculated the area occupied by the red pixels in the field. The nerve density was the nerve area divided by the total area examined ($\mu m^2/mm^2$). In Figure 1, the total nerve area was 1768 μm^2, whereas the total area examined was 0.1464 mm^2. Therefore, the nerve density was 12077 $\mu m^2/mm^2$.

Protocol 2

As will be presented in the Results section, protocol 1 showed increased ventricular vulnerability to fibrillation when hearts were perfused in room temperature and that both serum cholesterol and triglyceride levels were elevated. To demonstrate increased vulner-

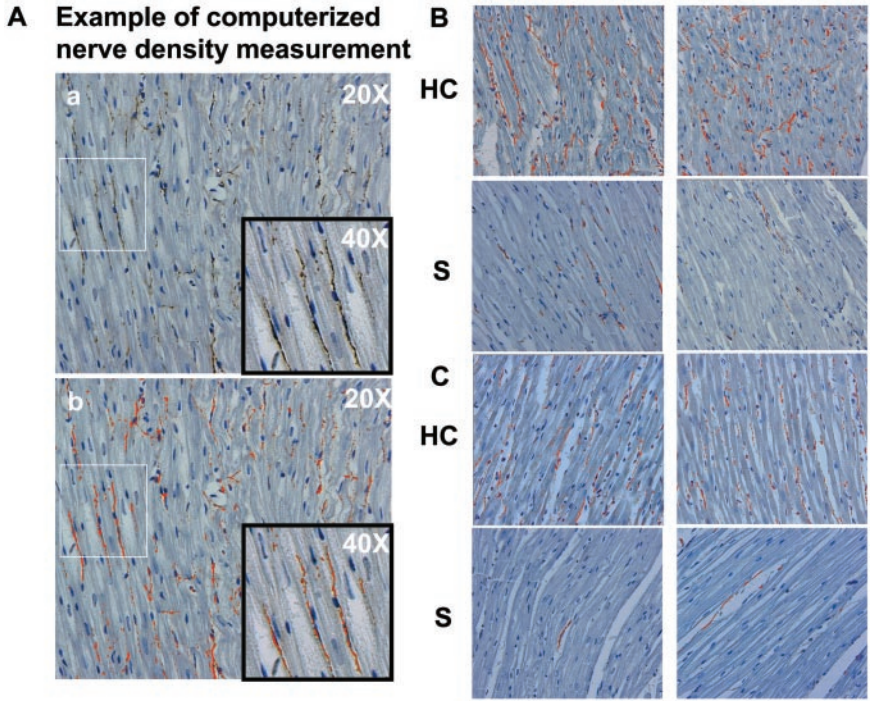

Figure 1. A, Example of computerized nerve density measurement. B and C, Examples of immunocytochemical staining of cardiac nerves with anti-GAP43 antibody (B) and with anti-TH antibody (C). Two rabbits each from HC and S groups were used.

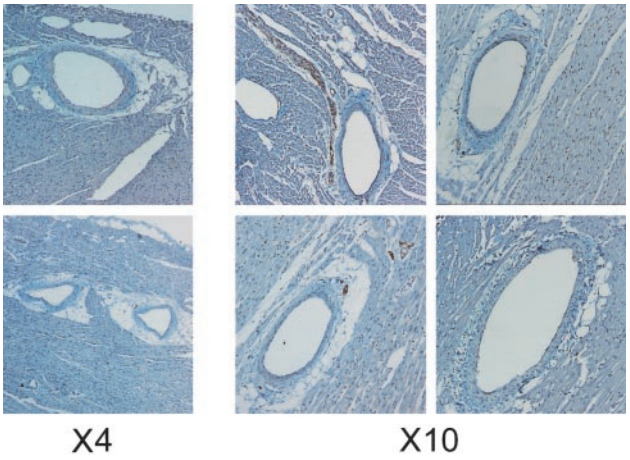

Figure 2. Examples of epicardial coronary arteries in HC rabbits stained with hematoxylin and GAP43. These 6 specimens came from 3 rabbits. Magnification of the objective lens was ×4 or ×10 (as labeled). None of these arteries showed significant coronary atherosclerosis. No myocardial infarction was observed. Nerves were stained brown.

ability at body temperature of rabbits with elevated cholesterol but normal triglyceride levels, we performed studies using protocol 2.

This protocol was conducted in the vivarium of Cedars-Sinai Medical Center. Rabbits were fed with high-cholesterol chow (HC group, n=12) or standard chow (S group, n=10) for a duration 1/3 shorter than the feeding duration in protocol 1 (8 weeks). We also reduced the coconut oil in the HC diet to 5%. All rabbits except 2 in the S group were female. All rabbit hearts were Langendorff-perfused with 37°C Tyrode's solution. Optical mapping studies were done to determine the action potential durations (APDs) at pacing cycle lengths (PCL) of 400, 300, and 200 ms. The optical mapping setup was similar to that reported in a previous study.[14] The tissues were stained with 0.5 μmol/L di-4-ANEPPS (Molecular Probes). An electromechanical uncoupler, 5 μmol/L cytochalasin D (Sigma Inc), was used. Laser light of 532-nm wavelength (Verdi, Coherent Inc) illuminated the tissues, and epifluorescence was collected through a long-pass filter with a cutoff wavelength of 600 nm (R60, Nikon) and a high-speed charge-coupled device camera (420 frames/s, Model CA D1-0128T, Dalsa Inc). One hundred points over the ventricular anterior wall were selected for APD analysis. A computer algorithm automatically determined the APD_{80}. The standard deviation (SD) and the difference (between the longest and shortest APD_{80}) of APD_{80} were used to represent the APD dispersion.

The baseline electrophysiological studies were performed using the same methods as in protocol 1. After baseline studies, we gave 0.1 μmol/L isoproterenol and repeated programmed stimulations to induce arrhythmia. Pseudo-ECG was continuously recorded during the loading and washout phase of isoproterenol infusion.

Protocol 3

This protocol was also conducted at Cedars-Sinai Medical Center. To induce different levels of serum cholesterol, we fed the rabbits with the following 3 dietary protocols: 4 rabbits were fed with standard chow for 8 weeks; 3 rabbits were fed with high cholesterol chow for 8 weeks; and 3 rabbits were fed with high cholesterol chow for 6 weeks followed by standard chow for 2 weeks. Nine of the 10 rabbits were female. The immunocytochemical studies were performed using the same methods as in protocol 1.

Statistical Analysis

All values will be expressed as mean±SD. Between-group comparisons were made with Student's *t* test for continuous variables and with the Chi-square test for categorical variables. Statistical significance was defined as $P \leq 0.05$.

An expanded Materials and Methods section can be found in the online data supplement available at http://www.circresaha.org.

Results

Protocol 1

The serum cholesterol levels were significantly higher in the HC group than in the S group (2097±288 versus 59±9 mg/dL; $P<0.001$). The serum triglyceride levels were also significantly higher in the HC group than in the S group (202±44 versus 50±10 mg/dL; $P<0.001$).

Nerve Sprouting and Sympathetic Hyperinnervation

Significant neural remodeling occurred in the HC group. Figures 1B and 1C show examples of GAP43 and TH immunocytochemical staining. Both GAP43- and TH-positive nerves were more abundant in the HC group than

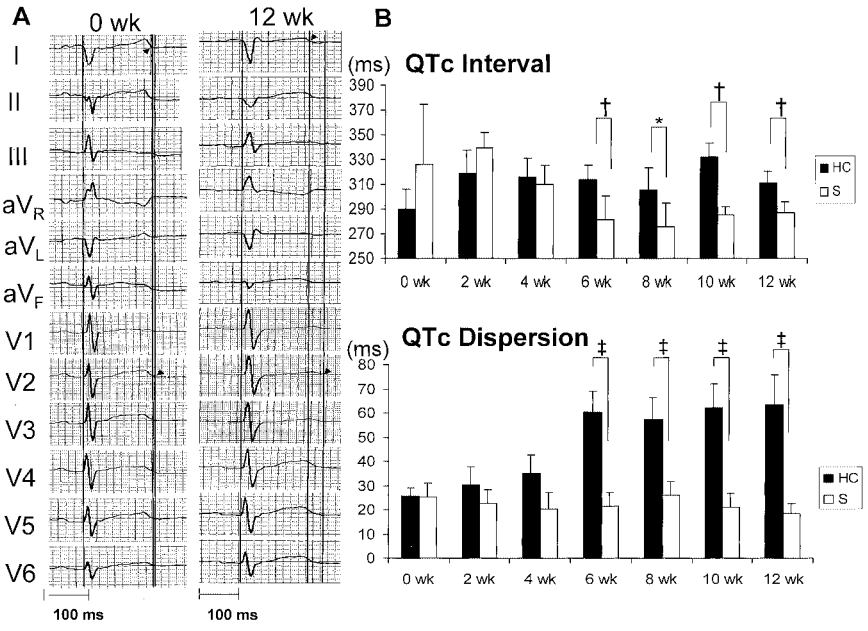

Figure 3. Measuring QT intervals. A, Examples of surface ECG in rabbits in HC group before and after 12 weeks of feeding. Vertical line segments indicate the time associated with the shortest and longest QT intervals. Arrowheads indicate the end of the shortest and longest T waves. End of the T wave was the point where T wave returned to the baseline. Time interval between these two vertical line segments is the QT dispersion. Sinus cycle length was 451 and 500 ms for the ECG before and after feeding, respectively. QTc was prolonged from 290 to 339 ms, whereas QTc dispersion increased from 22.3 to 63.6 ms after 12 weeks of feeding. B, Time-dependent changes in QTc interval and QTc dispersion in HC group and in S group. *$P<0.05$; †$P<0.01$; and ‡$P<0.001$.

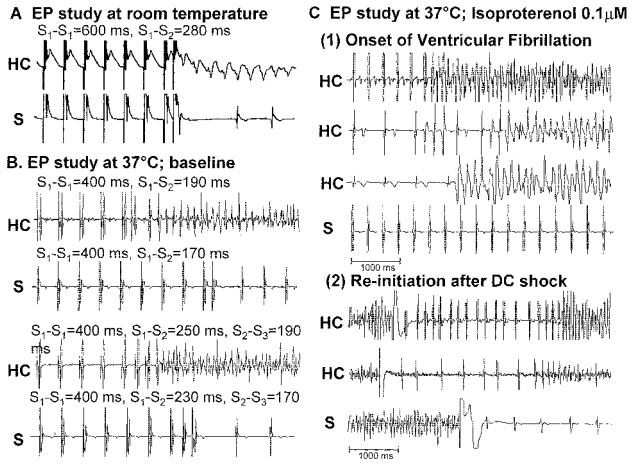

Figure 4. Induction of arrhythmia. A, At room temperature, ventricular tachyarrhythmia could be induced by a single premature ventricular stimulus in HC group but not in S group. B, At 37°C, ventricular tachyarrhythmia could be induced by single and double ventricular extrastimuli in HC group but not in S group. C, Under isoproterenol infusion, (1) spontaneous ventricular tachyarrhythmia occurred more frequently in HC group than S group, and (2) early recurrence of ventricular fibrillation after a successful shock was noted in HC group but not in S group.

in the S group. In the 12 rabbits (6 in each group) studied, GAP43- and TH-positive nerve densities were significantly higher in the HC group (5587±3747 and 2608±2592 $\mu m^2/mm^2$) than in the S group (2165±1443 and 462±687 $\mu m^2/mm^2$, respectively; $P<0.001$). There was no evidence of myocardial infarction in any of the specimens examined. In the HC group, minimal coronary atherosclerosis was observed in epicardial coronary arteries (Figure 2). Less than 10% of arterioles between myocardial muscle fibers had more than 50% luminal stenosis.

QTc Intervals and QTc Dispersion

The HC group showed significant QTc prolongation and increased QT dispersion. Figure 3A shows a typical example. The time-dependent changes in QTc interval and QTc dispersion of all rabbits studied is summarized in Figure 3B. The QTc interval was prolonged, and QTc dispersion was increased significantly in the HC group compared with the S group after 6 weeks. Before euthanasia, the HC group had a longer QTc interval (311±10 versus 287±9 ms; $P=0.001$) and more QTc dispersion (63.5±13 versus 18.5±4 ms; $P<0.001$) than the S group. There was no significant difference in the mean heart rate between groups during the first 10 weeks after feeding. However, the heart rate was lower in HC group than in S group at the 12th week after feeding (103.2±1.1/min versus 112.7±9.7/min; $P=0.049$).

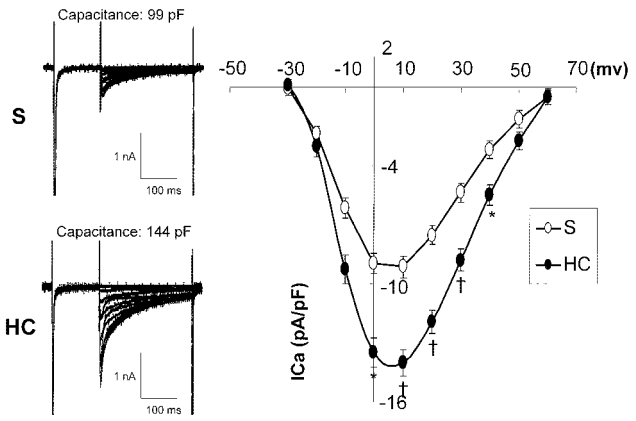

Figure 5. Current traces and *I*-V relationship of calcium inward currents in HC and S groups. Error bars represent SEM. *$P<0.05$; †$P<0.01$.

Ventricular Vulnerability to Fibrillation

The HC group showed increased vulnerability to fibrillation. Figure 4A shows the induction of ventricular tachyarrhythmia by a single premature ventricular stimulus in the HC group but not in the S group at room temperature. The sustained ventricular tachyarrhythmias either occurred spontaneously at the initiation of Langendorff's perfusion (2 rabbits) or could be induced by programmed stimulation (5 rabbits) in 77% (7/9) of HC group, whereas only in 11% (1/9) of the S group ($P<0.001$).

Calcium Inward Currents

The I_{Ca} in 8 cardiac myocytes of the HC (n=3) group and 13 cardiac myocytes of the S (n=3) group was compared and the current-voltage relationship determined (Figure 5). The peak I_{Ca} density was significantly higher in HC myocytes compared with S myocytes (14.0±3.1 versus 9.1±3.4 pA/pF; $P<0.01$). There was an insignificant increase in the capacitance (145±37 versus 123±46 pF; $P=0.26$) of HC myocytes, consistent with the increased average heart weight in the HC group.

Protocol 2

The serum cholesterol was significantly higher in the HC group than in the S group (1889±577 versus 50±21 mg/dL; $P<0.001$). The serum triglyceride levels were 100±90 mg/dL in HC group and 39±7 mg/dL in S group (P=NS). The average heart weight in the HC group was greater than that in S group (17.6±3.2 versus 15±1.9 g; $P=0.04$). However, the body weight was lower in the HC group compared with the S group (3.8±0.4 versus 4.5±0.9 kg; $P=0.01$).

APD, APD Dispersion, and the Effective Refractory Period

The HC group showed significant APD prolongation and increased APD dispersion after 8 weeks of feeding. Figure 6A shows typical examples of action potentials in 2 rabbits of each group at a PCL of 400 ms. The alterations in APD_{80} and APD_{80} dispersion are summarized in Figure 6B. The mean APD_{80} of the anterior wall at a PCL of 400 ms was significantly longer in the HC group than the S group (APD_{80}, 193±21 versus 174±17 ms; $P<0.05$). The longest APD_{80} of anterior wall in the HC group was significantly increased compared with S group at all 3 PCLs. The spatial heterogeneity of APD, represented as either the SD of APD_{80} at 100 points or the difference between the longest and shortest APD_{80} over the anterior wall, was also significantly greater in HC group compared with the S group (at PCL=400 ms: SD, 8.7±2.9 versus 5.5±2.0 ms; $P<0.01$; difference, 44.7±16.9 versus 25.1±7.3 ms; $P<0.01$). Meanwhile, the effective refractory period was longer in the HC group than in the S group for both single and double ventricular extrastimuli

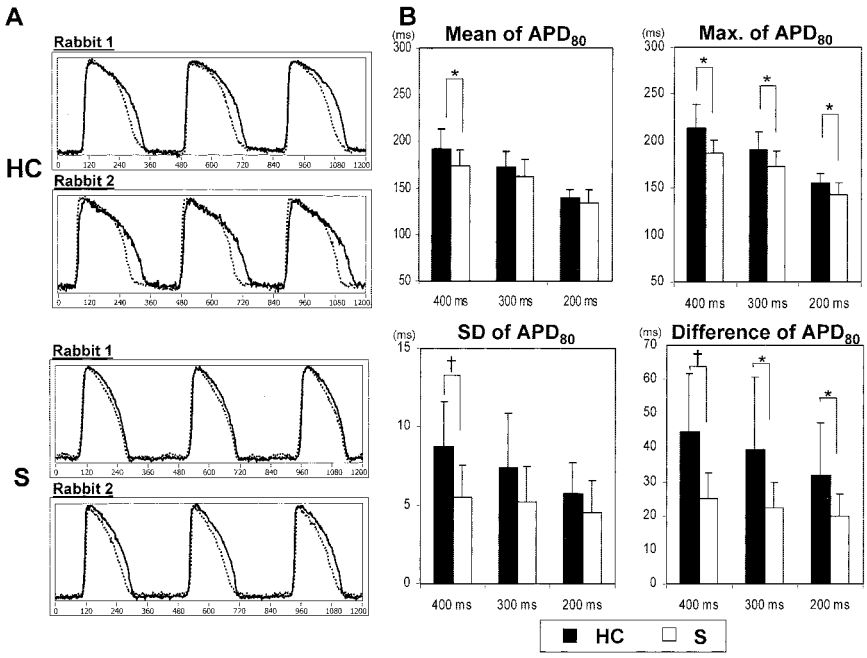

Figure 6. Action potential measured in protocol 2. A, Examples of action potentials at PCL of 400 ms in 2 rabbits of HC group and S group with shortest (dotted line) and longest (solid line) APD over anterior wall. B, Summary of the data obtained from 100 points over the anterior wall in HC and S groups. *$P<0.05$; †$P<0.01$.

(single, 192±12 versus 177±12 ms; $P=0.01$; double, 185±11 versus 168±20 ms; $P=0.02$).

Ventricular Vulnerability to Fibrillation

The HC group exhibited increased vulnerability to ventricular tachyarrhythmia at room temperature (Figure 4A). Furthermore, Figure 4B shows that sustained ventricular fibrillation could be induced by programmed ventricular stimulations in the HC group (3/12) but not in the S group (0/10) at 37°C. Under isoproterenol infusion, 58% (7/12) of the HC group and 20% (2/10) of the S group developed ventricular fibrillation (Figure 4C-1). Altogether, ventricular fibrillation was observed in 75% (9/12) of the HC group and 20% (2/10) of the S group ($P=0.01$). The Table shows the details of each ventricular fibrillation induction. Furthermore, 71% (5/7) of the HC group but none in S group experienced early recurrence of ventricular fibrillation (Figure 4C-2) after a successful defibrillation shock.

Protocol 3

The results of this protocol are summarized in Figure 7. Varying the diets resulted in different serum cholesterol levels. There was a dose-response relationship between serum cholesterol level and nerve density of both GAP43- ($R^2=0.94$; $P<0.001$) and TH-positive ($R^2=0.91$; $P<0.001$) nerves.

Discussion

This study showed that HC induced significant nerve sprouting and sympathetic hyperinnervation, increased I_{Ca}, prolonged APD and QTc intervals, and increased repolarization dispersion in a rabbit model. The neural and electrophysio-

VF Episodes in Protocol 2

ID	Conditions Associated With VF Induction	Total VF Duration Before Successful Shock	Mean VF Cycle Length
S1	Loading phase of isoproterenol infusion	30 sec	53 ms
S2	Washout phase of isoproterenol infusion	30 sec	46 ms
HC1	Spontaneous	30 sec	99 ms
	Washout phase of isoproterenol infusion	58 sec	98 ms
HC2	Programmed stimulation	86 sec	69 ms
HC3	Programmed stimulation	82 sec	117 ms
HC4	Loading and washout phase of isoproterenol infusion	15 min	45 ms
HC5	Loading and washout phase of isoproterenol infusion	25 min	43 ms
HC6	Loading phase of isoproterenol infusion	5 min	63 ms
HC7	Loading phase of isoproterenol infusion	135 sec	65 ms
HC8	Washout phase of isoproterenol infusion	3.5 min	104 ms
HC9	Washout phase of isoproterenol infusion	11 min	49 ms

VF indicates ventricular fibrillation; S1 and S2, rabbits fed with standard chow; HC1 through HC9, rabbits fed with HC chow. Rabbits without VF were not listed in the Table.

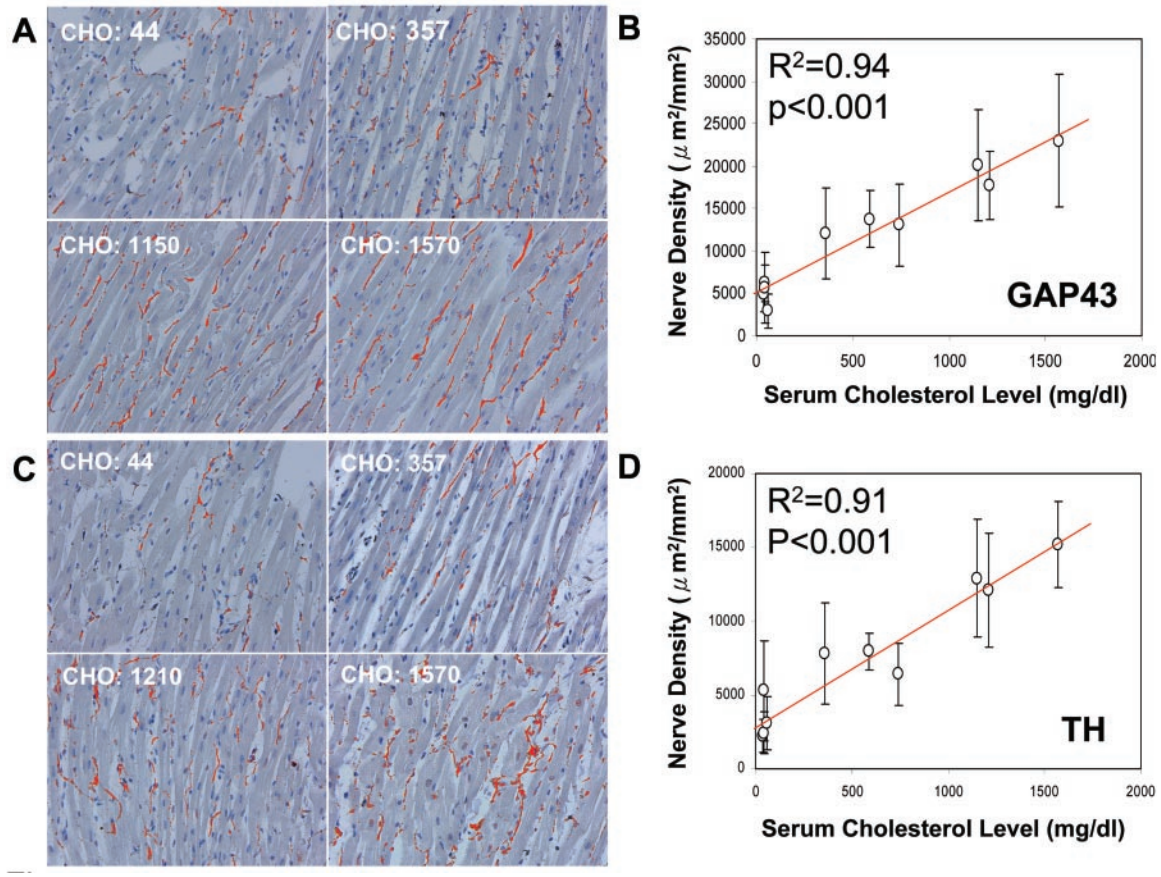

Figure 7. Nerve density and serum cholesterol levels. A, Examples of immunostaining results with anti-GAP43 antibody. Nerves are labeled red. B, Correlation between nerve density ($\mu m^2/mm^2$) and serum cholesterol level (mg/dL) for GAP43-positive nerves. C, Examples of immunostaining results with anti-TH antibody. D, Correlation between nerve density and serum cholesterol level for TH-positive nerves.

logical remodeling induced by HC was associated with increased ventricular vulnerability to fibrillation.

Mechanisms of Nerve Sprouting in Rabbits With Hypercholesterolemia

In both human and animal studies, HC was associated with increased oxidative stress.[15,16] Oxidative stress can cause neurodegeneration, neurite retraction, and mitochondrial dysfunction of the neurons in the central nervous system.[17] It is possible that oxidative stress causes cardiac nerve injury, which triggers the reexpression of nerve growth factor or other neurotrophic factor genes in the nonneural cells around the site of injury,[18–20] leading to nerve regeneration through nerve sprouting.[8,21,22] A second possible mechanism is that the increased circulating cholesterol directly triggers nerve sprouting. Transport of cholesterol and phospholipids is important in the repair, growth, and maintenance of myelin and neuronal membranes during development or after injury in the peripheral nerve system.[23,24] A dysfunction of the lipid-transport system is associated with compensatory sprouting and synaptic remodeling.[23] In cultured rabbit dorsal root ganglion neurons, incubation with β-very low-density lipoprotein, which are rich in apolipoprotein E (ApoE) and cholesterol, increases neurite outgrowth and branching.[25] Unesterified cholesterol added to the cultures had a similar, but less pronounced, effect. In the mouse model, the apolipoprotein, ApoE or ApoJ, upregulated after nerve injury and this coordinated alteration in apolipoproteins may redistribute lipid material to sprouting fibers to promote neurite extension.[26] In studies on rat retinal ganglion cells, synaptogenesis in the central nervous system is promoted by glia-derived cholesterol.[9] This latter study suggests that HC might directly stimulate nerve growth in the central nervous system. In the present study, we extended these observations into the peripheral nervous system and showed that HC in rabbits can also cause of cardiac nerve sprouting and sympathetic hyperinnervation through mechanisms unrelated to external nerve growth factor infusion, myocardial infarction, or electrical stimulation.[8,11,27]

Nerve Sprouting and Hypertrophy

Sympathetic hyperinnervation may also underlie the mechanisms of cardiac hypertrophy. In transgenic mice, overexpression of NGF in the heart caused both sympathetic hyperinnervation and cardiac enlargement.[28] NGF infusion in dogs could induce significant ventricular hypertrophy.[27] In the present study, the heart weight in the HC group was greater than the heart weight in the S group. These findings are consistent with the observation that chronic β-adrenergic stimulation can result in cardiac hypertrophy and cardiomyopathy.[29]

HC and Electrical Remodeling

In addition to nerve sprouting, HC apparently can directly remodel membrane currents. Our previous work revealed that

the sodium current density was significantly lower in the HC cardiac sarcolemma than in controls.[10] We also showed in the present study that the I_{Ca} was increased in rabbits with HC. The increased I_{Ca} could directly contribute to the increased QT intervals and APD prolongation observed in our study. Others[30] reported that excess free fatty acids could induce APD prolongation of canine Purkinje fibers and ovine false tendons.

It had been reported that the QTc interval became shorter with maturation in human and cultured neonatal rat ventricular myocytes.[31,32] It is possible that the progressive QT shortening in the control group is in part due to increasing age or an alteration of T-wave axis, which has complicated the correct QT measurements. However, in HC group of protocol 1, the QTc interval became longer as the rabbits aged. In addition to lengthening the QT interval in protocol 1, we also found that HC lengthened APD in protocol 2. In the latter protocol, the APD was measured with optical mapping techniques using objective computerized criteria. Taken together, we propose that HC indeed resulted in increased APD and QT intervals in this rabbit model.

Dietary lipid intake could modulate the membrane ionic currents by one of the following three mechanisms. First, an alteration in membrane fluidity could affect the function of the membrane-bound enzyme activity, such as Ca^{2+}- Mg^{2+} ATPase.[33] Secondly, the modification in dietary lipids could induce an alteration in the availability of fatty acid substrates and the balance of thromboxane A_2 and prostacyclin.[34] Thirdly, a direct lipid-protein interaction might affect the function of the ion channels and enzymes. The polyunsaturated fatty acids could directly bind to the Na^+-channel proteins and modify its function.[35] Incorporation of cholesterol into the isolated cardiac sarcolemmal vesicles could also stimulate the Na^+-Ca^{2+} exchange activity.[36]

Interaction Between Electrical Remodeling and Neural Remodeling

In addition to electrical remodeling, sympathetic hyperinnervation might also contribute to the proarrhythmic effects of HC. β-Adrenergic stimulation is known to increase ionic current through L-type calcium channels, potassium channels (I_{Ks}), and chloride channels ($I_{Cl(Ca)}$ and $I_{Cl\text{-}cAMP}$).[37,38] The increased outward currents tend to shorten APD, whereas the increased I_{Ca} tends to prolong APD. In normal canine ventricles in vivo, sympathetic stimulation results in shortening of APD and decreasing dispersion of refractoriness.[39] However, in electrically remodeled ventricles, sympathetic stimulation may prolong APD and increase APD dispersion.[40,41] The findings in our study are consistent with the proarrhythmic effects of sympathetic stimulation observed in remodeled ventricles.

Increased Ventricular Vulnerability to Fibrillation in Hypercholesterolemia

Spatial heterogeneity of repolarization is affected by preexisting anatomical heterogeneity, such as transmural APD dispersion and local anisotropy related to fiber orientation, or is dynamically modified by the restitution properties of APD and conduction velocity.[42] Increases in ventricular repolarization dispersions in diseased conditions were thought to be responsible for the life-threatening arrhythmias.[43] The APD and QTc dispersion were increased in rabbit hearts with HC in our study. Because hypothermia further enhanced the spatial heterogeneities of repolarization,[44] it resulted in a significant increase in the vulnerability to ventricular fibrillation in the HC group. Sympathetic stimulations could result in increased repolarization heterogeneity in hearts with heterogeneous sympathetic innervation or d-sotalol–induced APD prolongation.[45,46] In rabbit hearts with HC, sympathetic nerve sprouting may exaggerate the heterogeneity of innervation and electrical remodeling prolongs APD. It is possible that sympathetic stimulation in rabbit hearts with HC would further increase the repolarization dispersion and facilitate reentry formation. Meanwhile, prolongation of APD, increased I_{Ca} and sympathetic stimulation in rabbit hearts with HC could lead to increased intracellular calcium, which appears to be the common denominator in the generation of triggered activity.[47] Triggered activity after sympathetic stimulation in hearts with HC might underlie the spontaneous occurrence of ventricular fibrillation and early recurrence after a successful shock in our study.

Study Limitations

Protocol 1 was done in a different institution than the other two protocols. Due to the differences in genetic background, composition of the feeding chow and the feeding schedules of the vivariums, it is not possible to compare the nerve densities between protocol 1 and the other two protocols. We used optical mapping techniques to measure the APD and APD dispersion in the HC and S groups. Cytochalasin D was used as an excitation-contraction uncoupler in our study. Despite its low concentration, cytochalasin D had been reported to prolong the APD of the rabbits.[48] However, we treated the rabbit hearts of both groups with the same concentration of cytochalasin D. Therefore, the differences in APD and APD dispersion between the S and HC groups cannot be due to cytochalasin D alone. This conclusion is also strengthened by the QT interval measurements in protocol 1, which were made without the presence of cytochalasin D.

Acknowledgments

This study was supported by a National Taiwan University Hospital grant 89M011 to Dr Liu, a National Science Foundation (Taiwan) grant NSC88-2314-B-002-333 to Dr Wu, a National Health Research Institute (Taiwan) MD/DDS predoctoral fellowship DD9104C90 to Dr Lu, a Piansky endowment to Dr Fishbein, a Pauline and Harold Price endowment to Dr Chen, and by NIH grants P50-HL52319, R01-HL66389, R01-HL71140, and R01-HL58533, and the Ralph M. Parsons Foundation, Los Angeles, Calif. We thank Nina Wang and Elaine Lebowitz for their assistance.

References

1. The Long-Term Intervention with Pravastatin in Ischaemic Disease (LIPID) Study Group. Prevention of cardiovascular events and death with pravastatin in patients with coronary heart disease and a broad range of initial cholesterol levels. *N Engl J Med*. 1998;339:1349–1357.
2. LaRosa JC, He J, Vupputuri S. Effect of statins on risk of coronary disease: a meta-analysis of randomized controlled trials. *JAMA*. 1999; 282:2340–2346.
3. Randomised trial of cholesterol lowering in 4444 patients with coronary heart disease: the Scandinavian Simvastatin Survival Study (4S). *Lancet*. 1994;344:1383–1389.

4. De Sutter J, Tavernier R, De Buyzere M, Jordaens L, De Backer G. Lipid lowering drugs and recurrences of life-threatening ventricular arrhythmias in high-risk patients. *J Am Coll Cardiol*. 2000;36:766–772.
5. Gould KL. Reversal of coronary atherosclerosis: clinical promise as the basis for noninvasive management of coronary artery disease. *Circulation*. 1994;90:1558–1571.
6. Pinto JM, Boyden PA. Electrical remodeling in ischemia and infarction. *Cardiovasc Res*. 1999;42:284–297.
7. Cao J-M, Fishbein MC, Han JB, Lai WW, Lai AC, Wu T-J, Czer L, Wolf PL, Denton TA, Shintaku IP, Chen P-S, Chen LS. Relationship between regional cardiac hyperinnervation and ventricular arrhythmia. *Circulation*. 2000;101:1960–1969.
8. Cao J-M, Chen LS, KenKnight BH, Ohara T, Lee M-H, Tsai J, Lai WW, Karagueuzian HS, Wolf PL, Fishbein MC, Chen P-S. Nerve sprouting and sudden cardiac death. *Circ Res*. 2000;86:816–821.
9. Mauch DH, Nagler K, Schumacher S, Goritz C, Muller EC, Otto A, Pfrieger FW. CNS synaptogenesis promoted by glia-derived cholesterol. *Science*. 2001;294:1354–1357.
10. Wu CC, Su MJ, Chi JF, Chen WJ, Hsu HC, Lee YT. The effect of hypercholesterolemia on the sodium inward currents in cardiac myocyte. *J Mol Cell Cardiol*. 1995;27:1263–1269.
11. Chang C-M, Wu T-J, Zhou S-M, Doshi RN, Lee M-H, Ohara T, Fishbein MC, Karagueuzian HS, Chen P-S, Chen LS. Nerve sprouting and sympathetic hyperinnervation in a canine model of atrial fibrillation produced by prolonged right atrial pacing. *Circulation*. 2001;103:22–25.
12. Meiri KF, Pfenninger KH, Willard MB. Growth-associated protein, GAP-43, a polypeptide that is induced when neurons extend axons, is a component of growth cones and corresponds to pp46, a major polypeptide of a subcellular fraction enriched in growth cones [published erratum appears in *Proc Natl Acad Sci U S A*. 1986;83:9274]. *Proc Natl Acad Sci U S A*. 1986;83:3537–3541.
13. Chen P-S, Chen LS, Cao JM, Sharifi B, Karagueuzian HS, Fishbein MC. Sympathetic nerve sprouting, electrical remodeling and the mechanisms of sudden cardiac death. *Cardiovasc Res*. 2001;50:409–416.
14. Lin S-F, Roth BJ, Wikswo JP Jr. Quatrefoil reentry in myocardium: an optical imaging study of the induction mechanism. *J Cardiovasc Electrophysiol*. 1999;10:574–586.
15. Nourooz-Zadeh J, Smith CC, Betteridge DJ. Measures of oxidative stress in heterozygous familial hypercholesterolaemia. *Atherosclerosis*. 2001; 156:435–441.
16. Hsu HC, Lee YT, Chen MF. Effects of fish oil and vitamin E on the antioxidant defense system in diet-induced hypercholesterolemic rabbits. *Prostaglandins Other Lipid Mediat*. 2001;66:99–108.
17. de la Monte SM, Neely TR, Cannon J, Wands JR. Oxidative stress and hypoxia-like injury cause Alzheimer-type molecular abnormalities in central nervous system neurons. *Cell Mol Life Sci*. 2000;57:1471–1481.
18. Levi-Montalcini R. Growth control of nerve cells by a protein factor and its antiserum. *Science*. 1964;143:105–110.
19. Rush RA. Immunohistochemical localization of endogenous nerve growth factor. *Nature*. 1984;312:364–367.
20. Lindholm D, Heumann R, Meyer M, Thoenen H. Interleukin-1 regulates synthesis of nerve growth factor in non-neuronal cells of rat sciatic nerve. *Nature*. 1987;330:658–659.
21. Guth L. Regeneration in the mammalian peripheral nervous system. *Physiol Rev*. 1956;36:441–478.
22. Vracko R, Thorning D, Frederickson RG. Fate of nerve fibers in necrotic, healing, and healed rat myocardium. *Lab Invest*. 1990;63:490–501.
23. Poirier J. Apolipoprotein E in animal models of CNS injury and in Alzheimer's disease. *Trends Neurosci*. 1994;17:525–530.
24. Vancea JE, Campenotb RB, Vancec DE. The synthesis and transport of lipids for axonal growth and nerve regeneration. *Biochim Biophys Acta*. 2000;1486:84–96.
25. Handelmann GE, Boyles JK, Weisgraber KH, Mahley RW, Pitas RE. Effects of apolipoprotein E, β-very low density lipoproteins, and cholesterol on the extension of neurites by rabbit dorsal root ganglion neurons in vitro. *J Lipid Res*. 1992;33:1677–1688.
26. White F, Nicoll JA, Horsburgh K. Alterations in ApoE and ApoJ in relation to degeneration and regeneration in a mouse model of entorhinal cortex lesion. *Exp Neurol*. 2001;169:307–318.
27. Zhou S, Cao JM, Tebb ZD, Ohara T, Huang HL, Omichi C, Lee MH, KenKnight BH, Chen LS, Fishbein MC, Karagueuzian HS, Chen P-S. Modulation of QT interval by cardiac sympathetic nerve sprouting and the mechanisms of ventricular arrhythmia in a canine model of sudden cardiac death. *J Cardiovasc Electrophysiol*. 2001;12:1068–1073.
28. Hassankhani A, Steinhelper ME, Soonpaa MH, Katz EB, Taylor DA, Andrade-Rozental A, Factor SM, Steinberg JJ, Field LJ, Federoff HJ. Overexpression of NGF within the heart of transgenic mice causes hyperinnervation, cardiac enlargement, and hyperplasia of ectopic cells. *Dev Biol*. 1995;169:309–321.
29. Vatner DE, Asai K, Iwase M, Ishikawa Y, Shannon RP, Homcy CJ, Vatner SF. β-Adrenergic receptor-G protein-adenylyl cyclase signal transduction in the failing heart. *Am J Cardiol*. 1999;83:80H–85H.
30. Karagueuzian HS, Pennec JP, Deroubaix E, de Leiris J, Coraboeuf E. Effects of excess free fatty acids on the electrophysiological properties of ventricular specialized conducting tissue: a comparative study between the sheep and the dog. *J Cardiovasc Pharmacol*. 1982;4:462–468.
31. Rautaharju PM, Zhou SH, Wong S, Calhoun HP, Berenson GS, Prineas R, Davignon A. Sex differences in the evolution of the electrocardiographic QT interval with age. *Can J Cardiol*. 1992;8:690–695.
32. Meiry G, Reisner Y, Feld Y, Goldberg S, Rosen M, Ziv N, Binah O. Evolution of action potential propagation and repolarization in cultured neonatal rat ventricular myocytes. *J Cardiovasc Electrophysiol*. 2001;12: 1269–1277.
33. Muzulu SI, Bing RF, Norman RI. Human erythrocyte membrane fluidity and calcium pump activity in primary combined hyperlipidaemia. *Clin Sci (Lond)*. 1995;88:307–310.
34. Charnock JS, McLennan PL, Abeywardena MY. Dietary modulation of lipid metabolism and mechanical performance of the heart. *Mol Cell Biochem*. 1992;116:19–25.
35. Kang JX, Leaf A. Evidence that free polyunsaturated fatty acids modify Na^+ channels by directly binding to the channel proteins. *Proc Natl Acad Sci U S A*. 1996;93:3542–3546.
36. Kutryk MJ, Pierce GN. Stimulation of sodium-calcium exchange by cholesterol incorporation into isolated cardiac sarcolemmal vesicles. *J Biol Chem*. 1988;263:13167–13172.
37. Zygmunt AC. Intracellular calcium activates a chloride current in canine ventricular myocytes. *Am J Physiol*. 1994;267:H1984–H1995.
38. Hume JR, Harvey RD. Chloride conductance pathways in heart. *Am J Physiol*. 1991;261:C399–C412.
39. Takei M, Sasaki Y, Yonezawa T, Lakhe M, Aruga M, Kiyosawa K. The autonomic control of the transmural dispersion of ventricular repolarization in anesthetized dogs. *J Cardiovasc Electrophysiol*. 1999;10: 981–989.
40. Shimizu W, Antzelevitch C. Cellular basis for the ECG features of the LQT1 form of the long-QT syndrome: effects of beta-adrenergic agonists and antagonists and sodium channel blockers on transmural dispersion of repolarization and torsade de pointes. *Circulation*. 1998;98:2314–2322.
41. Shimizu W, Antzelevitch C. Differential effects of β-adrenergic agonists and antagonists in LQT1, LQT2 and LQT3 models of the long QT syndrome. *J Am Coll Cardiol*. 2000;35:778–786.
42. Wolk R, Cobbe SM, Hicks MN, Kane KA. Functional, structural, and dynamic basis of electrical heterogeneity in healthy and diseased cardiac muscle: implications for arrhythmogenesis and anti-arrhythmic drug therapy. *Pharmacol Ther*. 1999;84:207–231.
43. Amlie JP. Dispersion of repolarization: a basic electrophysiological mechanism behind malignant arrhythmias. *Eur Heart J*. 1997;18: 1200–1202.
44. Salama G, Kanai AJ, Huang D, Efimov IR, Girouard SD, Rosenbaum DS. Hypoxia and hypothermia enhance spatial heterogeneities of repolarization in guinea pig hearts: analysis of spatial autocorrelation of optically recorded action potential durations. *J Cardiovasc Electrophysiol*. 1998; 9:164–183.
45. Yoshioka K, Gao DW, Chin M, Stillson C, Penades E, Lesh M, O'Connell W, Dae M. Heterogeneous sympathetic innervation influences local myocardial repolarization in normally perfused rabbit hearts. *Circulation*. 2000;101:1060–1066.
46. Spear JF, Moore EN. Modulation of arrhythmias by isoproterenol in a rabbit heart model of D-sotalol-induced long Q-T intervals. *Am J Physiol Heart Circ Physiol*. 2000;279:H15–H25.
47. Volders PG, Vos MA, Szabo B, Sipido KR, de Groot SH, Gorgels AP, Wellens HJ, Lazzara R. Progress in the understanding of cardiac early afterdepolarizations and torsades de pointes: time to revise current concepts. *Cardiovasc Res*. 2000;46:376–392.
48. Banville I, Gray RA. Effect of action potential duration and conduction velocity restitution and their spatial dispersion on alternans and the stability of arrhythmias. *J Cardiovasc Electrophysiol*. 2002;13: 1141–1149.

Materials and Methods

All animal study protocols were approved by the Animal Care and Use Committee of the respective institutions and conformed to the guidelines of the American Heart Association. Three-month-old New Zealand white rabbits were used for the study. Total Serum cholesterol and triglyceride levels were determined by automated enzymatic methods (Merck; 14366 and 14354, respectively) before the animals were sacrificed.

Protocol 1

This protocol was conducted in the vivarium of National Taiwan University School of Medicine, Taipei, Taiwan. Rabbits were fed with high fat and cholesterol chow (HC group, N=10) or standard chow (S group, N=10) for 12 weeks. Purina 5321 (St. Louis, MO, USA) was used as standard rabbit chow. In HC chow, 40% of the total energy source was derived from 0.5% cholesterol (Wako Co., Japan) and 10% coconut oil (Yeali Co., Taiwan). The salt and vitamin mix met the standards of the American Institute of Nutrition. In each group, 3 rabbits were male and 7 rabbits were female. All female rabbits had bilateral oophorectormy performed at the age of 2 months. The rabbits were enrolled into the study when they reached 3 months of age.

Twelve-Lead Electrocardiographic study

Twelve-lead surface electrocardiograms (ECGs) were performed in 6 rabbits of each group at 2-week intervals for 12 weeks. After anesthetization with intramuscular ketamine and xylazine, electrocardiograms were recorded at a paper speed of 50 mm/s and a voltage calibration of 0.5 mV/cm. QT interval was measured manually from the onset of the QRS complex to the end of the T wave. QT dispersion was defined as the

difference between the longest and the shortest QT interval in the 12-lead ECG. In the case of a flat T wave or if a P wave distorted the end of the preceding T wave at fast heart rates, the duration of the QT interval could not be measured. ECG recordings with <9 measurable QT intervals on the 12-lead ECG were excluded from QT-dispersion analyses. The QTc was the QT divided by the square root of the RR interval in seconds.

Isolated Rabbit Heart Preparation and Electrophysiological Study

Rabbits were anesthetized with intravenous pentobarbital (50 mg/kg) or with intravenous ketamine (20 mg/Kg) and xylazine (5 mg/Kg). The chests were opened via median sternotomy. The hearts were quickly removed and Langendorff perfused with Tyrode's solution at room temperature (25° to 28°C). The Tyrode's solution had the following composition (in mM): 125 NaCl, 4.5 KCl, 0.25 $MgCl_2$, 24 $NaHCO_3$, 1.8 NaH_2PO_4, 1.8 $CaCl_2$, and 5.5 glucose. The pH was maintained at 7.4, and the solution was continuously oxygenated with 95% O_2 and 5% CO_2. Coronary perfusion pressure was regulated between 80 and 95 mmHg and the hearts were exposed to air. Pseudo-ECG registered with a widely spaced bipole was used to monitor heart rhythm. Electrical stimuli were delivered through the bipolar catheter with a rectangular pulse of 2-ms duration and 2 mA current (3-5 times the diastolic threshold). The vulnerability to ventricular tachyarrhythmias was tested with a single S_2 given after 8 S_1 at a cycle length of 600 ms on both left and right ventricles. If the intrinsic cycle length was shorter than 600 ms, we would clamp the sinus node to slow down the rate. The premature coupling intervals were initially paced at 480 ms, then shortened successively in steps of 20ms while PCL>300 ms and in steps of 10ms when PCL<300ms until the effective refractory period was reached or when fibrillation was induced.

Whole-Cell Clamping Study for Calcium Current measurement

Single cell isolation was performed as previously described.[1] Briefly, 3 hearts of each group were retrogradely perfused with Ca^{2+}-free Tyrode's solution at 37°C for 5 mins, followed by enzymatic digestion with type II collagenase (0.25 mg/ml, Sigma, St. Louis, Mo., USA) and type XIV protease (0.05mg/ml, Sigma). Afterwards the hearts were perfused with Kraftbruhe (KB) solution containing (in mM): taurine 10, glutamic acid 70, KCl 25, KH_2PO_4 10, dextrose 22, EGTA 0.5, titrated with KOH to pH 7.3 for 5 min. Tissues from the left ventricle were dispersed in KB solution at room temperature (~25°C). Only rod-like, Ca^{2+}-tolerant cells with clear striation were used for the experiment. The cardiomyocytes were transferred to a chamber mounted on an inverted microscope (Nikon Diaphot, Nikon Co., Japan) for electrophysiologic recording. Currents were recorded at room temperature with a Dagon 8900 amplifier, filtered at 10 kHz with four-pole Bessel filter, digitized at 20 μsec intervals, and stored using a Digidata-1200 analog-to-digital interface along with pClamp software (Axon Instruments, Foster City, CA). The input resistance of glass electrodes was 2-5 MΩ in all experiments. Junctional potentials were electronically compensated before seal formation. Whole-cell configuration was obtained after impalement of the cell. Capacitance transients were electronically compensated, and the cells were allowed to dialyze with internal solution for 10 min. During measurement of calcium current (ICa), the potassium current was prevented with the presence of Cs^+ in both external and internal solution. The internal solution contained (in mM): CsCl 130, EGTA 5, tetraethylammonium chloride 15, cAMP 0.03, dextrose 5, HEPES-CsOH buffer (pH 7.4) 10. The external solution contained (in mM): NaCl 137.0, KCl 5.4, CsCl 1, $CaCl_2$ 1.8, $MgCl_2$ 1.1, Dextrose 11, HEPES 10,

titrated to pH 7.4 with NaOH. A two-step depolarization protocol with a holding potential of -80 mV was used to study ICa. After depolarization to -40 mV for 100 ms (to inactivate the sodium channel), ICa was evoked by a second 300-ms depolarization to a test potential between –30 mV to 60 mV. The amplitude of ICa was measured as the peak amplitude of inward current. Data were then converted to current densities (pA/pF) according to cell capacitance.

Immunocytochemical Study

Ventricular tissues of rabbit hearts were fixed by 4% formalin for 1h followed by 70% alcohol for more than 48h after electrophysiological studies. Ventricles were cross-sectioned from apex to base. Three sections of each heart were used for immunocytochemical studies. Details of the staining techniques have been published elsewhere.[2,3] Briefly, we used anti-growth-associated protein 43 (GAP43) and anti-tyrosine hydroxylase (TH) antibodies for immunocytochemical staining. GAP43, a protein expressed in the growth cones of sprouting axons,[4] is a marker for nerve sprouting. TH is a marker of sympathetic nerves. We determined nerve density by a computer-assisted image analysis system (Image-Pro Plus 4.0). Each slide was examined under a microscope with 20X objectives. In each quadrant of the slide, we selected one microscopic field with the highest nerve density. The computer automatically detected the stained nerves in these fields by their brown color (Figure 1A-a) and then labeled these nerves with a red color on the computer screen (Figure 1A-b). We then inspected the tagged picture and manually removed incorrectly selected objects before counting. The computer then calculated the area occupied by the red pixels in the field. The nerve density was the nerve area divided by the total area examined ($\mu m^2/mm^2$). In Figure 1,

the total nerve area was 1768 μm^2 while the total area examined was 0.1464 mm^2. Therefore, the nerve density was 12077 $\mu m^2/mm^2$.

Protocol 2

As will be presented in the Results section, Protocol 1 showed increased ventricular vulnerability to fibrillation when hearts were perfused in room temperature and that both serum cholesterol and triglyceride levels were elevated. To demonstrate increased vulnerability at body temperature of rabbits with elevated cholesterol but normal triglyceride levels, we performed studies using Protocol 2.

This protocol was conducted in the vivarium of Cedars-Sinai Medical Center. Rabbits were fed with high cholesterol chow (HC group, N=12) or standard chow (S group, N=10) for a duration 1/3 shorter than the feeding duration in Protocol 1 (8 weeks). We also reduced the coconut oil in the HC diet to 5%. All rabbits except 2 in the S group were female. All rabbit hearts were Langendorff-perfused with 37°C Tyrode's solution. Optical mapping studies were done to determine the action potential durations (APDs) at pacing cycle lengths (PCL) of 400, 300 and 200 ms. The optical mapping setup was similar to that reported in a previous study.[5] The tissues were stained with 0.5 μM di-4-ANEPPS (Molecular Probes). An electromechanical uncoupler, 5 μM cytochalasin D (Sigma Inc.), was used. Laser light of 532-nm wavelength (Verdi, Coherent Inc.) illuminated the tissues, and epifluorescence was collected through a long-pass filter with a cutoff wavelength of 600 nm (R60, Nikon) and a high-speed charge-coupled device (CCD) camera (420 frames/s, Model CA D1-0128T, Dalsa Inc.). One hundred points over the ventricular anterior wall were selected for action potential duration (APD)

analysis. A computer algorithm automatically determined the APD_{80}. The standard deviation (SD) and the difference (between the longest and shortest APD_{80}) of APD_{80} were used to represent the APD dispersion.

The baseline electrophysiological studies were performed using the same methods as in Protocol 1. After baseline studies, we gave 0.1 μM isoproterenol and repeated programmed stimulations to induce arrhythmia. Pseudo-ECG was continuously recorded during the loading and washout phase of isoproterenol infusion.

Protocol 3

This protocol was also conducted at Cedars-Sinai Medical Center. To induce different levels of serum cholesterol, we fed the rabbits with the following 3 dietary protocols: Four rabbits were fed with standard chow (Purina 5321) for 8 weeks. Three rabbits were fed with high fat and cholesterol chow (Purina 5321+0.5% cholesterol+5% coconut oil) for 8 weeks. Three rabbits were fed with high fat and cholesterol chow for 6 weeks followed by standard chow for 2 weeks. Nine of the 10 rabbits were female. The immunocytochemical studies were performed using the same methods as in Protocol 1.

Statistical Analysis

All values will be expressed as mean ± SD. Between-group comparisons were made with Student's t-test for continuous variables and with the Chi-square test for categorical variables. Statistical significance was defined as $p \leq 0.05$.

References

1. Wu CC, Su MJ, Chi JF, Chen WJ, Hsu HC, Lee YT. The effect of hypercholesterolemia on the sodium inward currents in cardiac myocyte. *J Mol Cell Cardiol*. 1995;27:1263-1269.

2. Cao J-M, Chen LS, KenKnight BH, Ohara T, Lee M-H, Tsai J, Lai WW, Karagueuzian HS, Wolf PL, Fishbein MC, Chen P-S. Nerve sprouting and sudden cardiac death. *Circ Res*. 2000;86:816-821.

3. Chang C-M, Wu T-J, Zhou S-M, Doshi RN, Lee M-H, Ohara T, Fishbein MC, Karagueuzian HS, Chen P-S, Chen LS. Nerve sprouting and sympathetic hyperinnervation in a canine model of atrial fibrillation produced by prolonged right atrial pacing. *Circulation*. 2001;103:22-25.

4. Meiri KF, Pfenninger KH, Willard MB. Growth-associated protein, GAP-43, a polypeptide that is induced when neurons extend axons, is a component of growth cones and corresponds to pp46, a major polypeptide of a subcellular fraction enriched in growth cones [published erratum appears in Proc Natl Acad Sci U S A 1986 Dec;83(23):9274]. *Proc Natl Acad Sci U S A*. 1986;83:3537-3541.

5. Lin S-F, Roth BJ, Wikswo JP, Jr. Quatrefoil reentry in myocardium: an optical imaging study of the induction mechanism. *J Cardiovasc Electrophysiol*. 1999;10:574-586.